

**Electrically driven singularity and control of carrier spin of a hybrid quantum well**Pilkyung Moon,<sup>1,\*</sup> Won Jun Choi,<sup>2</sup> and J. D. Lee<sup>1</sup><sup>1</sup>*School of Materials Science, Japan Advanced Institute of Science and Technology, Asahidai 1-1, Nomi, Ishikawa, Japan 923-1292*<sup>2</sup>*Nano Convergence Devices Center, Interdisciplinary Fusion Technology Division, Korea Institute of Science and Technology, 39-1 Hawolgok, Seoungbuk, Seoul, Korea 136-791*

(Received 17 March 2011; published 29 April 2011)

We propose a hybrid quantum well structure comprising a compressively strained layer and tensile-strained layer and find that the major band character of the valence band maximum can be switched between the heavy hole of the compressively strained layer and the light hole of the tensile-strained layer by application of an electric field. Remarkably, in the switching resonant region, we find that the  $g$  factors of both heavy-hole and light-hole states become singular (i.e., there is discontinuous change between positive and negative extrema), which enables the extreme control of the hole spin of the hybrid quantum well by the electric field.

DOI: [10.1103/PhysRevB.83.165450](https://doi.org/10.1103/PhysRevB.83.165450)

PACS number(s): 75.70.Cn, 73.21.Fg, 73.61.Ey, 75.70.Tj

**I. INTRODUCTION**

Spin states of confined carriers (i.e., electrons or holes) are promising candidates for logical units in quantum computations.<sup>1</sup> The manipulation of the spin states and/or corresponding  $g$  factor, which is the measure of the spin splitting by a magnetic field, is one of the most challenging problems in semiconductor spintronics.<sup>2</sup> So far, the spin up and down states are mainly manipulated by controlling the external magnetic field. However, it is difficult to control the magnetic field on a reduced length scale. This also makes it difficult to integrate such a magnetically controlled device on a small scale. Therefore, the electrical control of spin states is highly desirable for the implementation of quantum gate operations. DiVincenzo *et al.* proposed a theoretical device in which quantum information is stored in the carrier spin, whose order can be reversed by electrically shifting the carrier from a material with a low  $g$  factor to one with a high  $g$  factor.<sup>3</sup> This proposition opened up a new field of spintronics and provided a practical option to incorporate the external electric field for manipulation of the spin states in nanoscopic building blocks. Another possibility of controlling spin states with an electric field using the orbital mechanism (i.e., the Rashba effect) was also proposed.<sup>4,5</sup>

The intuitive scheme of shifting the carrier wave function and resultant electrical control of  $g$  factors has been widely applied to various nanoscopic systems. It has been implemented in a single quantum well (QW) (e.g., GaAs/AlGaAs heterostructure<sup>6</sup> or  $\text{Al}_x\text{Ga}_{1-x}\text{As}$  QW with  $x$  gradually varying across the structure<sup>7</sup>) and a coupled QW (e.g., two separate QWs made from AlAs and  $\text{Al}_{0.1}\text{Ga}_{0.9}\text{As}$ <sup>8</sup>), a pair of undoped GaAs QWs with an  $\text{Al}_{0.33}\text{Ga}_{0.67}\text{As}$  barrier,<sup>9</sup> and InGaAs/InAlAs heterostructure with double InAs-inserted QWs.<sup>10</sup> The same scheme has also been applied to a coupled quantum dots system (e.g., vertically stacked InAs/GaAs quantum dot pairs<sup>11</sup>) and enabled the electrical control of the  $g$  factor for a single confined spin rather than that for an ensemble of carrier spins in QW. In addition, as alternative approaches, the orbital mechanism of spin control was experimentally demonstrated for InAs-based QWs<sup>12,13</sup> and the many-body correction of the exciton wave function in terms of the electric field in coupled QWs was suggested.<sup>14</sup>

In this paper, we propose a theoretical scheme for the electric-field-induced singularity in the hole  $g$  factor of a hybrid QW (HQW) and subsequently the extreme control of the spin states. The HQW under consideration is composed of asymmetric coupled double InGaAs/InP QWs comprising a compressively strained layer (CSL) and tensile-strained layer (TSL). The uppermost hole states of the HQW can be electrically switched between a heavy hole (HH) and light hole (LH) since the valence band maxima (VBM) of the CSL and TSL are an HH and LH, respectively. The  $g$  factors of HH and LH, or those of HH and LH excitons, are not only different in magnitude but also different in sign.<sup>15</sup> Therefore the HQW enables large changes of the  $g$  factors. In this proposition, by applying an electric field along the growth direction, the energy levels of HH and LH states can be tuned to resonance, and the HH spin up state and LH spin down state with Landau level quantum number  $\nu = 0$  would undergo singular anticrossing, while the HH spin down state and LH spin up state would not because of the absence of interaction. In particular, there would be a dramatic inversion of the order of HH and LH spin states leading to a singularity of the hole  $g$  factors (i.e., discontinuous change between positive and negative extrema) for the resonant electric field, and this would provide a new scheme for the extreme control of  $g$  factors distinguishable from the various electrical approaches introduced in this section.

**II. MODEL AND METHOD**

We schematically illustrate atomic distortions (strains) and valence band structures of a zinc blende material in Figs. 1(a)–1(c). Under a lattice-matched condition, HH and LH bands are degenerate at the zone center ( $k=0$ ), but LH bands are above HH bands in a tensile-strained material and vice versa in compressively strained materials.<sup>16</sup> Thus, the VBM of the CSL and TSL are an HH and LH, respectively. With a suitable choice of well width, one can energetically match the HH of the CSL and the LH of the TSL for any combination of materials for the CSL and TSL. In this study, we investigated the HQW composed of an  $\text{In}_{0.4}\text{Ga}_{0.6}\text{As}$  layer (as the TSL) and an  $\text{In}_{0.7}\text{Ga}_{0.3}\text{As}$  layer (as the CSL) grown on InP substrate. Figure 1(d) shows the eight bands near a fundamental gap of an  $\text{In}_x\text{Ga}_{1-x}\text{As}$  ( $0 \leq x \leq 1$ ) layer pseudomorphically grown on

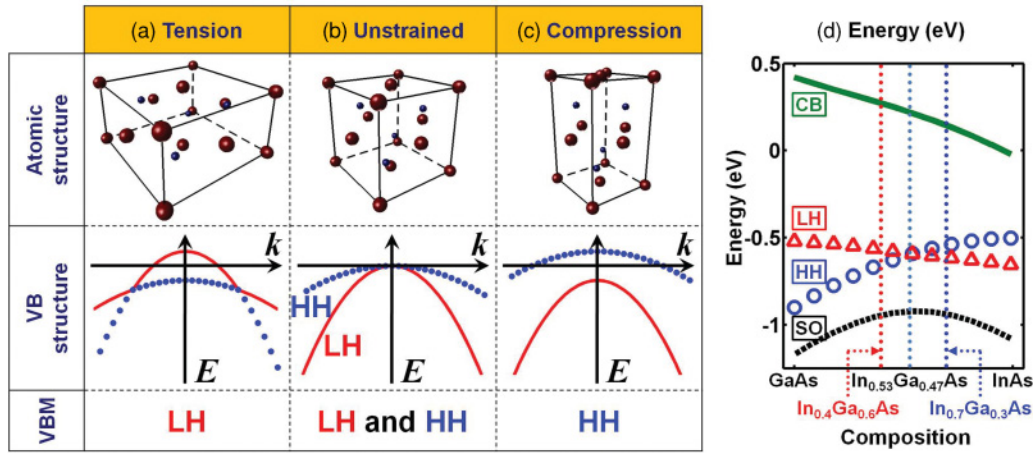


FIG. 1. (Color online) Schematic atomic distortions and valence band structures in the momentum space of a zinc blende material under (a) lateral tension, (b) lattice-matched (unstrained) condition, and (c) lateral compression. Red solid (blue dashed) lines in valence band (VB) structure represent the LH (HH) bands. Red solid (blue dashed) lines in VB structure represent the LH (HH) bands (d) Eight bands near a fundamental gap (green solid line: conduction bands (CB); blue circles: HH bands; red triangles: LH bands; black dashed line: spin-orbit (SO) split-off bands. Each band is doubly degenerate with spin up and down states) of an  $\text{In}_x\text{Ga}_{1-x}\text{As}$  ( $0 \leq x \leq 1$ ) layer pseudomorphically grown on InP. The vertical red (blue) dotted line indicates the band structure of  $\text{In}_{0.4}\text{Ga}_{0.6}\text{As}$  ( $\text{In}_{0.7}\text{Ga}_{0.3}\text{As}$ ).

InP. Materials with an In mole fraction  $x$  lower (higher) than 0.53 are under lateral tension (compression); thus, their LH bands are above (below) HH bands.

We use the eight-band  $k \cdot p$  Hamiltonian,

$$H = H_K + H_\varepsilon + H_{SO} + H_Z, \quad (1)$$

where  $H_K$  corresponds to the terms which depend on canonical momentum operator  $K_i = k_i + eA_i/\hbar$  ( $i = x, y, z$ ),  $k_i$  to the kinetic momentum operator,  $e > 0$  to the elementary charge,  $A_i$  to the electromagnetic vector potential,  $H_\varepsilon$  to the strain-dependent contribution,  $H_{SO}$  to the spin-orbit interaction, and  $H_Z$  to the Zeeman term. We use the Landau gauge  $(A_x, A_y, A_z) = (0, Bx, 0)$  to represent the magnetic field applied parallel to the growth direction ( $z$ ), and solve the Hamiltonian equation in a reciprocal space to eliminate the spurious solutions. The explicit form of the Hamiltonian matrix is detailed in the literature.<sup>17</sup> Each state is characterized by a quantum number  $n$ , and only the states with the same quantum number interact. Table I shows the relationship between the quantum number  $n$  and the Landau-level quantum number  $\nu$ . Figure 2 shows the strain-modified valence band potentials and the wave functions of the two lowest states (HH and LH states) of the HQW at zero bias in the absence of a magnetic field. The present HQW is designed as a 12-nm-thick  $\text{In}_{0.4}\text{Ga}_{0.6}\text{As}$  layer and a 2.5-nm-thick  $\text{In}_{0.7}\text{Ga}_{0.3}\text{As}$  layer. The thick red solid line in the figure shows the LH band edge potential profile, and the thick blue dashed line shows the HH band edge potential profile. The width and material composition of each well is

TABLE I. Landau-level quantum number  $\nu$  for spin up ( $\uparrow$ ) and down ( $\downarrow$ ) conduction band (CB), LH band, spin-orbit (SO) split-off band, and HH band for a given quantum number  $n$ .

	CB	LH	SO	HH
$\uparrow$	$n$	$n$	$n$	$n - 1$
$\downarrow$	$n + 1$	$n + 1$	$n + 1$	$n + 2$

chosen to make the HH ground state and LH ground state almost degenerate.

### III. RESULTS AND DISCUSSIONS

As in the aforementioned electrical approaches,<sup>6–11</sup> the degree of localization of the holes to either QW would depend on the external electric field (i.e., quantum-confined Stark effects), and thus, the  $g$  factors of HH and LH states can be changed by the field. However, the calculated energies of HH and LH spin states in Fig. 3 are more dramatic and interesting than expected. In Fig. 3, the energies of the four uppermost hole states (HH spin up and down states and LH spin up and down states) with  $\nu = 0$  at 1 T are given as functions of the magnitude of the external electric field. The ground state carrier is the HH of the CSL below the resonant electric field  $F_0$  ( $\approx -1.5$  kV/cm) and the LH of the TSL above  $F_0$ . In addition, for an electric field below  $-2.5$  kV/cm, the spin up states of both the HH

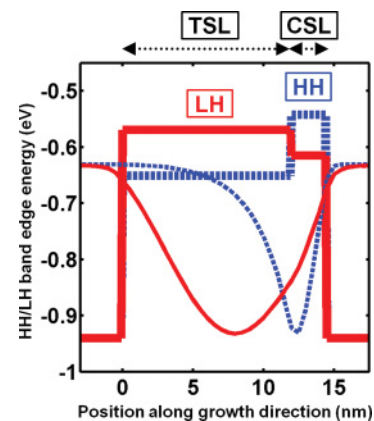


FIG. 2. (Color online) Strain-modified band-edge potential of HH (thick blue dashed line) and LH (thick red solid line), and the first two lowest states wave functions (HH: thin blue dashed line; LH: thin red dashed line) of the HQW at zero bias.

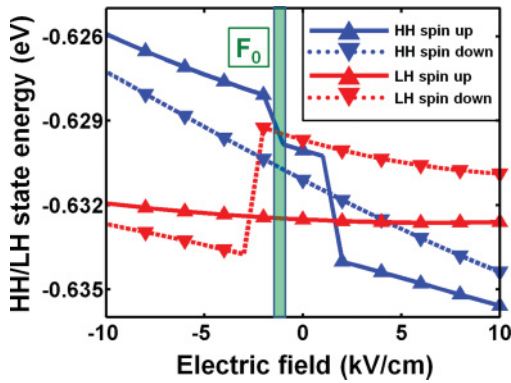


FIG. 3. (Color online) Energies of the four uppermost hole states (HH spin up and down states, and LH spin up and down states) with  $\nu = 0$  at 1 T. Blue solid (dashed) line with triangles pointing up (down) represents the HH spin up (down) state and red solid (dashed) line with triangles pointing up (down) indicates the LH spin up (down) state.  $F_0$  represents the electric field at which the uppermost HH and LH states cross each other.

and LH are above their corresponding spin down states, while for an electric field above 1.5 kV/cm, the spin down states of both the HH and LH are above their corresponding spin up states. The electric fields between  $-2.5$  and  $1.5$  kV/cm define a switching region of the HH and LH. Below the region, the ground and first excited hole states are the spin up and down states of the HH, and, above the region, they are the spin down and up states of the LH. It is worth noting that the center of the region is near the zero field (i.e.,  $F_0 \approx -1.5$  kV/cm) although it could, in principle, be tuned by a detailed design of the HQW. This implies that, just by changing the direction of the external electric field, not only the band characters of the two uppermost hole states but also the order of their spin up and down states can be abruptly changed.

One of the most interesting features of the HQW under consideration is that the spin splitting of both the HH and LH increases as the electric field approaches  $F_0$ . This can be clearly seen by the behavior of the  $g$  factor with respect to the electric field. The  $g$  factor is defined by

$$g_\nu(B) = \frac{E_{\nu,\uparrow} - E_{\nu,\downarrow}}{\mu_B B}, \quad (2)$$

which corresponds to the measure of the energy splitting between two states with the same  $\nu$  and opposite spin directions in the magnetic field  $B$ .  $E_{\nu,\uparrow}$  and  $E_{\nu,\downarrow}$  are the energies of the spin up and down states with  $\nu$ , respectively, and  $\mu_B$  is the Bohr magneton. The  $g$  factors for the HH (blue dashed line) and LH (red solid line) as functions of the electric field are displayed in Fig. 4. Large circles indicate the uppermost (i.e., ground) hole states in a given electric field and small circles the excited hole states. For the resonant field  $F_0$ , the  $g$  factors of both the HH and LH become singular. Remarkably, the  $g$  factors reach positive extrema of up to 40 at  $F_0 - \varepsilon$  and abruptly drop to negative extrema of  $-55$  at  $F_0 + \varepsilon$ , where  $\varepsilon$  is a small positive number. Recalling that  $F_0$  could, in principle, be tuned to zero with a suitable design of the HQW, a simple change in the electric field direction might induce a singular change in the  $g$  factor of  $O(10)$ . Such a dramatic change in the  $g$  factor has not ever been observed before.

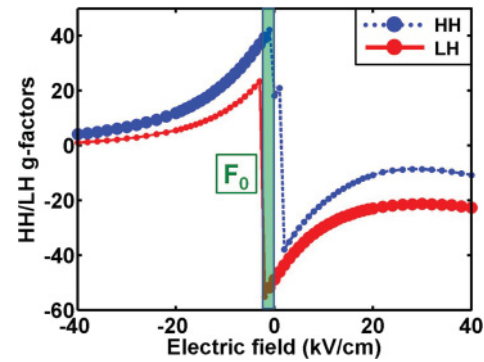


FIG. 4. (Color online) The  $g$  factors of the HH (blue dashed line) and LH (red solid line) states with  $\nu = 0$  at 1 T. Large circles indicate the uppermost (i.e., ground) hole states in a given electric field and small circles the excited hole states.  $F_0$  represents the electric field at which the uppermost HH and LH states cross each other.

The singularity of the  $g$  factors for the HH and LH near  $F_0$  can be explained by the anticrossing of HH and LH states. Figure 2 shows that the wave functions of the HH and LH for zero in-plane wave vectors do not interact with each other in the absence of a magnetic field. In the presence of a magnetic field, however, the HH and LH exhibit state mixing and anticrossing as the energies of the two states become closer. The singularity of the HH  $g$  factor originates from the discontinuous drop in energy of the HH spin up state near  $F_0$ . Table I shows that the HH spin up state with  $\nu = 0$  ( $n = 1$ ) interacts with the LH spin up state with  $\nu = 1$  ( $n = 1$ ) and the LH spin down state with  $\nu = 2$  ( $n = 1$ ). We plot the energies of the HH and LH with  $n = 1$  in Fig. 5(a). Each state is labeled with its major band character. Near the resonant electric field  $F_0$ , there is state mixing and anticrossing of the HH spin up state with  $\nu = 0$  and the LH spin up state with  $\nu = 1$  [and also the LH spin down state with  $\nu = 2$ , not explicitly shown in Fig. 5(a)] and finally interchange of the major band character. The energy of the HH spin up state with  $\nu = 0$  drops twice in the switching region. The first drop of the HH spin up state (at  $-1.5$  kV/cm) is because of the interaction with the LH spin down state with  $\nu = 2$ , and the second drop (at  $1.5$  kV/cm) is because of

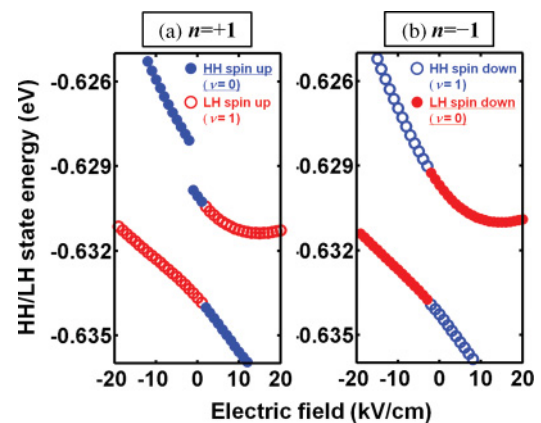


FIG. 5. (Color online) Energies of the HH and LH states with (a)  $n = 1$  and (b)  $n = -1$  at 1 T. Each state is labeled with its major band character (HH/LH).



the interaction with the LH spin up state with  $\nu = 1$ . On the contrary, since the HH spin down state with  $\nu = 0$  is the only one for which  $n = -2$ , it does not interact with any other state and has a nearly linear energy shift as the electric field increases (see Fig. 3). Therefore, it is understood that the singular HH  $g$  factor is attributed to this singular behavior of the HH spin up state in contrast to the monotonous HH spin down state. In the same way, the singularity and sign change of the LH  $g$  factor are understood. The energy of the LH spin down state with  $\nu = 0$  ( $n = -1$ ) abruptly drops at  $-2.5$  kV/cm owing to the interaction with the HH spin down state with  $\nu = 1$  ( $n = -1$ ) as shown in Fig. 5(b). In contrast, the LH spin up state with  $\nu = 0$  ( $n = 0$ ) is monotonous and smooth because it does not interact strongly with other nearby states (see Fig. 3).

It may be worth mentioning that, in Fig. 5, the values of the electric fields for the anticrossing of the states with  $n = 1$  and  $n = -1$  differ; the HH spin up state with  $n = 1$  has discontinuous energy drops at  $-1.5$  and  $1.5$  kV/cm, while the LH spin down with  $n = -1$  has a discontinuous energy drop at  $-2.5$  kV/cm. Accordingly, the values of the electric fields at which the  $g$  factors of HH and LH states change signs (see Fig. 4) slightly differ. The  $g$  factor of the HH state changes sign at  $1.5$  kV/cm, while that of the LH state changes at  $-2.5$  kV/cm.

This is the first theoretical proposal which manages the singularity of the hole  $g$  factor utilizing the HH-LH coupling. The pronounced resonance behavior associated with the anticrossing of HH and LH states suggests that it can be controlled with an external field and hence used in a similar fashion to the conventional spintronic device. We note that the state anticrossing can also be observed in another nanostructure. In a single tensile-strained QW, the LH ground state is expected to show a larger quantum-confined Stark shift than the HH first excited state when an electric field is applied so that the two states show an anticrossing behavior at an electric field high enough to offset the energy difference by Stark effect.<sup>18</sup>

In addition, it is also expected that similar anticrossing might occur in the system with  $\Gamma$  and X states depending on the interaction between those.<sup>8</sup> In those systems, however, the  $g$  factor behavior and its manipulation around such anticrossings are still unexplored problems. Nevertheless, it is stressed that the  $g$  factor manipulation under the state anticrossing would be a promising direction to realize the controllable nanoscopic spin unit for spintronics.

#### IV. CONCLUSION

In conclusion, we have proposed a theory for the electrical manipulation of the hole  $g$  factor of a HQW comprising a CSL and TSL. The HQW allows a spatial separation of the HH and LH states, thus enabling us to intuitively manipulate the relative energy levels of the HH states of the CSL and the LH states of the TSL. In particular, in terms of the electric field, the energy levels of the HH and LH states can be tuned to resonance, and state mixing and anticrossing achieved. Importantly, we have found that this leads to a dramatic inversion of the order of HH and LH spin states and subsequently the singularity of the hole  $g$  factors at the resonant field strength. Our finding provides a scheme for the extreme control of the  $g$  factor of the HQW, an excellent candidate for application to spintronic devices.

#### ACKNOWLEDGMENTS

This work was partially supported by Special Coordination Funds for Promoting Science and Technology from MEXT, Japan, and by the Converging Research Center Program through the Ministry of Education, Science, and Technology, Korea (Grant No. 2010K000971). P. M. would like to acknowledge the support from Korea Institute of Science and Technology Information Supercomputing Center through the strategic support program for the supercomputing application research (Grant No. KSC-2009-S02-0009).

\*pilkyung.moon@gmail.com

<sup>1</sup>D. Loss and D. P. DiVincenzo, *Phys. Rev. A* **57**, 120 (1998).

<sup>2</sup>S. A. Wolf, D. D. Awschalom, R. A. Buhrman, J. M. Daughton, S. von Molnár, M. L. Roukes, A. Y. Chtchelkanova, and D. M. Treger, *Science* **294**, 1488 (2001).

<sup>3</sup>D. P. DiVincenzo, G. Burkard, D. Loss, and E. V. Sukhorukov, in *Proceedings of NATO ASI on Quantum Mesoscopic Phenomena and Mesoscopic Devices in Microelectronics*, edited by I. O. Kulik and R. Ellialtioglu (Kluwer Academic, Dordrecht, 1999).

<sup>4</sup>A. B. Yu and E. I. Rashba, *J. Phys. C* **17**, 6039 (1984).

<sup>5</sup>E. I. Rashba and A. L. Efros, *Phys. Rev. Lett.* **91**, 126405 (2003).

<sup>6</sup>H. W. Jiang and E. Yablonovitch, *Phys. Rev. B* **64**, 041307 (2001).

<sup>7</sup>G. Salis, Y. Kato, K. Ensslin, D. C. Driscoll, A. C. Gossard, and D. D. Awschalom, *Nature (London)* **414**, 619 (2001).

<sup>8</sup>E. P. De Poortere and M. Shayegan, *Appl. Phys. Lett.* **84**, 3837 (2004).

<sup>9</sup>M. Poggio, G. M. Steeves, R. C. Myers, N. P. Stern, A. C. Gossard, and D. D. Awschalom, *Phys. Rev. B* **70**, 121305 (2004).

<sup>10</sup>Y. Lin, J. Nitta, T. Koga, and T. Akazaki, *Physica E: Low-dimensional Systems and Nanostructures* **21**, 656 (2004).

<sup>11</sup>M. F. Doty, M. Scheibner, I. V. Ponomarev, E. A. Stinaff, A. S. Bracker, V. L. Korenev, T. L. Reinecke, and D. Gammon, *Phys. Rev. Lett.* **97**, 197202 (2006).

<sup>12</sup>J. Nitta, T. Akazaki, H. Takayanagi, and T. Enoki, *Phys. Rev. Lett.* **78**, 1335 (1997).

<sup>13</sup>D. Grundler, *Phys. Rev. Lett.* **84**, 6074 (2000).

<sup>14</sup>G. Aichmayr, M. Jetter, L. Viña, J. Dickerson, F. Camino, and E. E. Mendez, *Phys. Rev. Lett.* **83**, 2433 (1999).

<sup>15</sup>Y. H. Chen, X. L. Ye, B. Xu, Z. G. Wang, and Z. Yang, *Appl. Phys. Lett.* **89**, 051903 (2006).

<sup>16</sup>P. Moon, K. Park, E. Yoon, and J. P. Leburton, *Phys. Status Solidi RRL* **3**, 76 (2009).

<sup>17</sup>A. Zakharova, S. T. Yen, and K. A. Chao, *Phys. Rev. B* **69**, 115319 (2004).

<sup>18</sup>Y. Kajikawa, *Phys. Rev. B* **49**, 8136 (1994).